AD-A069 599 AEROSPACE CORP EL SEGUNDO CALIF IVAN A GETTING LABS F/G 20/5
DESALE-5: A COMPREHENSIVE SCHEDULED MIXING MODEL FOR CW CHEMICA--ETC(U)
MAY 79 M EPSTEIN F04701-78-C-0079
UNCLASSIFIED TR-0079(4940-01)-3 SAMSO-TR-79-31 NL

| OF |
AD
A069599

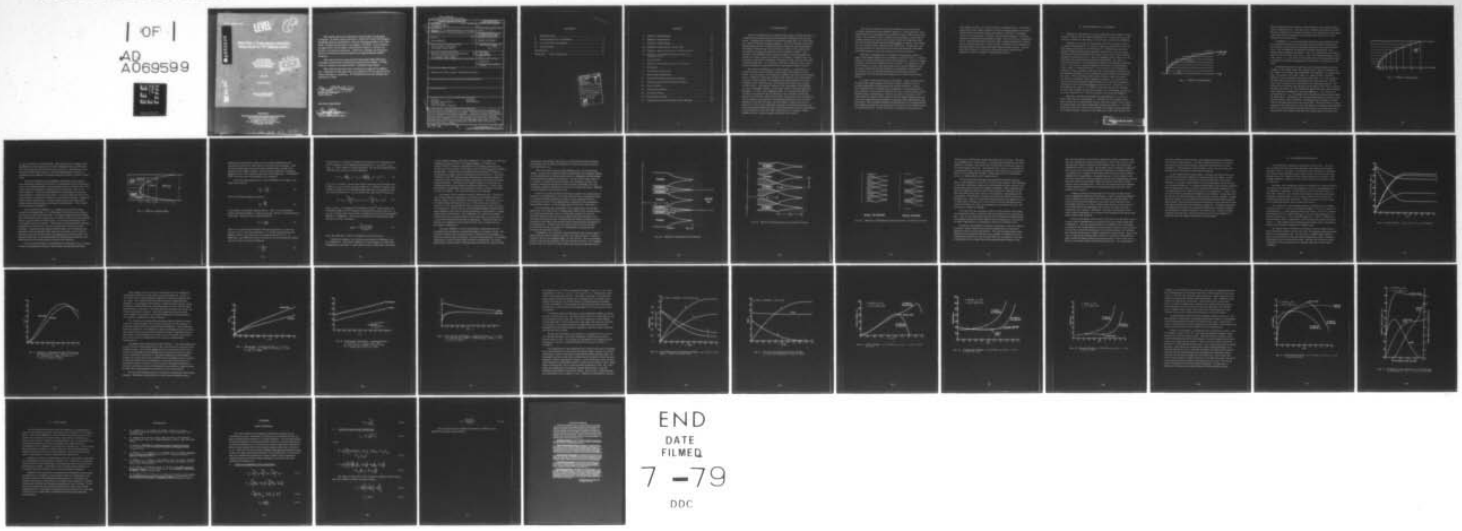

END
DATE
FILMED
7 -79
DDC

REPORT SAMSO-TR-78-31

LEVEL II

AD A069599

DESALE-5: A Comprehensive Scheduled Mixing Model for CW Chemical Lasers

MELVIN SPUCKLER
Aerophysics Laboratory
The Jonn A. Gosling Laboratories
The Aerospace Corporation
El Segundo, Calif. 90245

DDC
DEC 11 1978
C

1 May 1978

Interim Report

APPROVED FOR PUBLIC RELEASE;
DISTRIBUTION UNLIMITED

FILE COPY

Prepared for

SPACE AND MISSILE SYSTEMS ORGANIZATION
AIR FORCE SYSTEMS COMMAND
Los Angeles Air Force Station
P.O. Box 92960, Worldway Postal Center
Los Angeles, Calif. 90009

78 06 07 019

This interim report was submitted by The Aerospace Corporation, El Segundo, CA 90245, under Contract No. F04701-78-C-0079 with the Space and Missile Systems Organization, Contracts Management Office, P.O. Box 92960, Worldway Postal Center, Los Angeles, CA 90009. It was reviewed and approved for The Aerospace Corporation by Walter R. Warren, Jr., Director, Aerophysics Laboratory. Gerhard E. Aichinger was the project officer for Mission-Oriented Investigation and Experimentation (MOIE) Programs.

This report has been reviewed by the Information Office (OI) and is releasable to the National Technical Information Service (NTIS). At NTIS, it will be available to the general public, including foreign nations.

This technical report has been reviewed and is approved for publication. Publication of this report does not constitute Air Force approval of the report's findings or conclusions. It is published only for the exchange and stimulation of ideas.

Gerhard E. Aichinger
Project Officer

FOR THE COMMANDER

Frank J. Bane, Chief
Contracts Management Office

UNCLASSIFIED

SECURITY CLASSIFICATION OF THIS PAGE (When Data Entered)

REPORT DOCUMENTATION PAGE	READ INSTRUCTIONS BEFORE COMPLETING FORM
1. REPORT NUMBER: SAMSO-TR-79-31	2. GOVT ACCESSION NO.
3. RECIPIENT'S CATALOG NUMBER	
4. TITLE (and Subtitle): DESALE-5: A COMPREHENSIVE SCHEDULED MIXING MODEL FOR CW CHEMICAL LASERS	5. TYPE OF REPORT & PERIOD COVERED: Interim rept.
6. PERFORMING ORG. REPORT NUMBER: TR-0079(4940-01)-3	
7. AUTHOR(s): Melvin/Epstein	8. CONTRACT OR GRANT NUMBER(s): F04701-78-C-0079
9. PERFORMING ORGANIZATION NAME AND ADDRESS: The Aerospace Corporation, El Segundo, Calif. 90245	10. PROGRAM ELEMENT, PROJECT, TASK AREA & WORK UNIT NUMBERS: 45 p.
11. CONTROLLING OFFICE NAME AND ADDRESS: Space and Missile Systems Organization, Air Force Systems Command, Los Angeles, Calif. 90009	12. REPORT DATE: 1 May 1979
	13. NUMBER OF PAGES: 43
14. MONITORING AGENCY NAME & ADDRESS (if different from Controlling Office)	15. SECURITY CLASS. (of this report): Unclassified
	15a. DECLASSIFICATION/DOWNGRADING SCHEDULE

16. DISTRIBUTION STATEMENT (of this Report)

Approved for public release; distribution unlimited

17. DISTRIBUTION STATEMENT (of the abstract entered in Block 20, if different from Report)

18. SUPPLEMENTARY NOTES

19. KEY WORDS (Continue on reverse side if necessary and identify by block number)

Blockage
Boundary-Layer Effects
Chemical Laser
Laser Computer Programs
Modeling
Reacting Flow

20. ABSTRACT (Continue on reverse side if necessary and identify by block number)

The development and application of a comprehensive model for calculating cw chemical laser performance are described. The effects of mixing through the use of a scheduled mass addition algorithm, extensive modeling of the pertinent chemical reactions, Fabry-Perot optics, nozzle blockage, and nonuniform initial profiles resulting from nozzle boundary layers are given. Illustrative examples are provided to demonstrate the capability of the model to treat these various phenomena. A typical running time on a CDC 7600 is 30 to 60 sec with all of the effects modeled.

DD FORM 1473 (FACSIMILE)

UNCLASSIFIED 409 944

SECURITY CLASSIFICATION OF THIS PAGE (When Data Entered)

CONTENTS

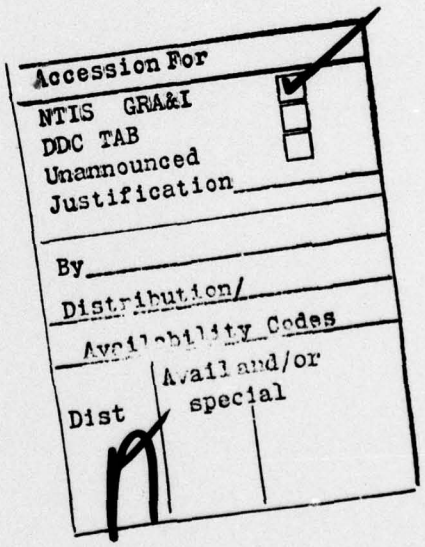

FIGURES

I. INTRODUCTION

Since the invention of the cw chemical laser about a decade ago (Ref. 1), considerable effort has been directed toward the modeling of laser performance. Although some analytical work has been done (Ref. 2), for the most part, this work has been mainly qualitative. The focus has been primarily on defining the primary scaling parameters pertinent to laser performance. That this work has been at all successful is a tribute to the insight of the investigators, because the problem is extraordinarily complex. For example, in the HF(DF) system, detailed computer calculations typically include more than 15 species and about 150 reactions. Furthermore, it is necessary to specify the temperature dependence of the reaction rates of the chemical system (Ref. 3) as well as, in the more elaborate codes, multicomponent diffusion coefficients for the various species (Refs. 4 and 5).

The need for modeling is, of course, obvious. A model that is as complete and accurate as possible is desireable in the design of a laser device. In recent years, very elaborate computer codes have been developed that are capable of treating the chemistry and mixing in great detail (Refs. 3, 4, and 5). In these models, the handling of the chemical kinetics is fairly straightforward, limited only by uncertainties in the important reactions and their rates. An adequate treatment of the mixing part of the problem is a more formidable problem. In the early codes, mixing was neglected altogether. In codes such as RESALE (Ref. 3), it was assumed that the reactants were premixed and not allowed to react until they reached the entrance to the optical cavity; at which time, the reactions were switched on. The gas mixture was assumed to be uniformly distributed in the direction transverse to the flow direction, and all transport in that direction was neglected. It was soon verified that at pressures of practical interest, not only was mixing an important factor in the determination of laser performance, but nonuniformities in the flow that resulted from, for example, nozzle boundary layers, could also significantly affect the results.

The earliest attempts to account for mixing were focused on the so-called "programmed mass addition" approach. In this approach, only a small portion of the reactants were permitted to react at the entrance to the cavity. The remainder of the reactants were permitted to mix in with the resultant products of reaction as the gases flowed on through the cavity. The rate of mass addition was prescribed a priori in a manner that related the rate of mixing to the conditions at the nozzle exit. Furthermore, the reacting mixture was still assumed to flow one dimensionally with either prescribed pressure or area as a function of the flow direction x.

This type of modeling was very helpful in clarifying the effects of many of the complex phenomena occurring in a real laser device. It further helped to verify the usefulness of some of the analytical results and, equally important, some of the limitations of those results. The simplicity of this type of model, of course, had associated with it certain ambiguities, not the least of which was the specification of an appropriate mixing length. The obvious way to avoid these problems was to develop a fully two-dimensional code that included the mixing process in all of its pertinent details.

A number of such codes have been developed. They are based on the boundary-layer approximation to the Navier-Stokes equations and are generally applicable to both laminar and turbulent flow (Refs. 4 and 5). These models allow for sophisticated consideration of nonuniformities of flow properties in the direction normal to flow as a result of mixing, nozzle boundary layers, and blockage. Whereas a number of questions can be raised about the details of these models, they are highly sophisticated state-of-the-art models and are not likely to be improved upon significantly in the near future. They certainly constitute a great advance over the programmed mass addition models and are much preferred models for the detailed design of a particular device. On the other hand, compared to the programmed

mass addition models, they require lengthy computation times. This feature makes these codes rather expensive for such important applications as parametric studies, experiment design and analysis, definition of operating regimes for various types of devices, and sensitivity analyses. For these purposes, programmed mass addition models, with much shorter computation times, would be preferable if they were able to handle satisfactorily some of the two-dimensional effects. Until recently, nonuniform initial profiles and blockage effects were outside the scope of these simpler models. The purpose of this report is to describe a programmed mass addition code, DESALE-5, which is capable of treating these effects.

II. DEVELOPMENT OF THE MODEL

DESALE-5 is the latest in a line of programmed mass addition models that have evolved from the original RESALE code. A convenient way to describe its evolution is, therefore, to describe its evolution from RESALE.

RESALE is a strictly one-diminsional code for a premixed pulsed or cw chemical lasing system. It, in turn, began as a modification of the one-dimensional reacting flow code NEST (Ref. 6). RESALE was derived by adding to NEST the appropriate radiation equations to account for lasing. The optical cavity was assumed to be formed from a pair of plane-parallel partially transmitting mirrors. Since the emphasis in this report is on the modeling of the fluid mechanical aspect of the problem, the reader is referred to Reference 3 for the details of radiation and chemistry modeling. Here, it will suffice to state that RESALE is a strictly one-dimensional code in which it is assumed that at $x = 0$ a set of premixed reactants are permitted to begin reacting. With this code, the variation of all but one of the dependent variables can be calculated as the gas mixture flows through the cavity. These variables include all the fluid mechanical variables, the chemistry variables, and the radiation variables. As a result of the nature of the one-dimensional approximation, one of the fluid mechanical variables has to be specified a priori as a function of x. In practice, it is generally the flow area A. It is often of interest to specify the variation of some other variable such as the pressure p or, occasionally, the density ρ, or the temperature T. Each can, and has, been done with RESALE.

DESALE-1 was the first attempt to modify RESALE to account for some of the effects of mixing (Ref. 7). The point of view adopted at that time was that the reaction started, in fact, not at the entrance to the cavity, but along a flame sheet that contained the reaction zone (Fig. 1). The shape of the flame sheet was chosen to be parabolic for laminar mixing and linear for turbulent mixing. (Because of the small scale of the laser nozzles and

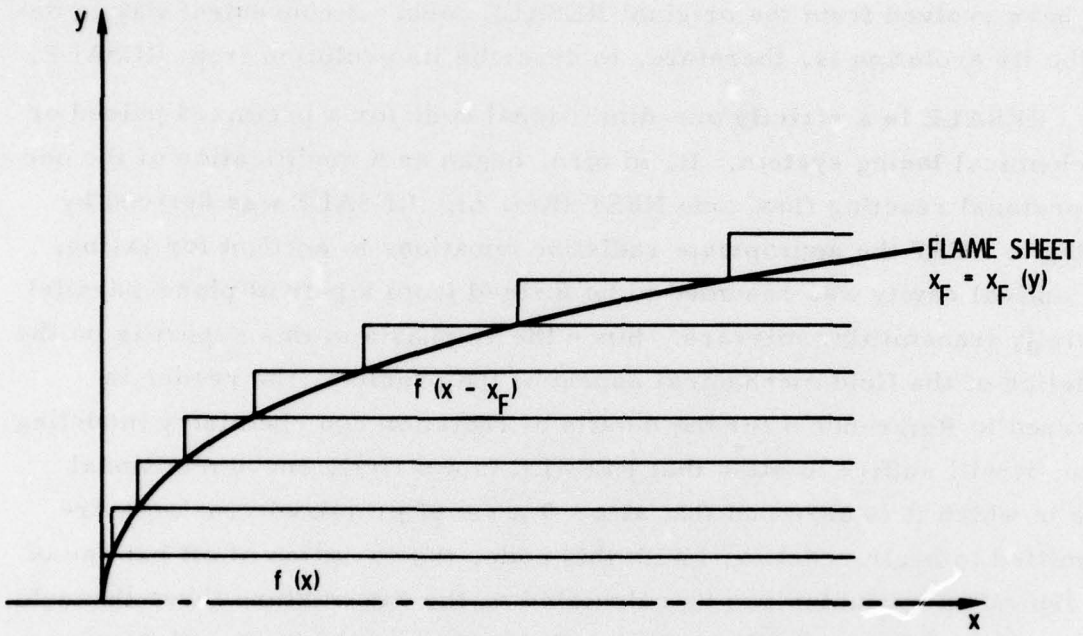

Fig. 1. DESALE-1 Mixing Model

the low pressures characteristic of chemical lasers, only laminar mixing will be considered here.) Note that, since conditions upstream of the flame sheet are considered to be known and uniform, the specification of the shape of the flame sheet is equivalent to the specification of the rate of mass addition to the reaction zone.

In DESALE-1, it was assumed that each stream tube experienced the same variations of fluid mechanical and chemical variables with distance, the origin for each stream tube being the point where it crossed the flame sheet. The variations of the dependent variables with distance were obtained from a RESALE calculation. Thus, for a stream line at a height y, which crosses the flame sheet at $x_F = x_F(y)$, any dependent variable f varies with x as $f(x - x_F)$. The laser radiation extracted in this approximation then is obtained as a suitable averaging in the y direction across all the stream tubes.

Although this model accounted for some of the qualitative effects of mixing, it was rather crude and, except for the case of constant pressure flows, was fraught with ambiguities. For example, in constant area flow, the pressure at a given value of x varied in the y direction. DESALE-2 was developed to improve the model (Ref. 7). It was based on the flame-sheet concept also, but differed in an important way. In this model, the reactants were assumed also to be uniformly premixed. The stream tube nearest the axis was assumed to begin to react when it reached the flame sheet (Fig. 2). The solution for that stream tube was determined by the application of RESALE, just as in DESALE-1. The solution was calculated up to $x = x_1$, the position where the adjacent stream tube crossed the flame sheet. At that point, the reactants and products of reaction in the first stream tube were assumed to mix instantaneously (without reaction) with the reactants from the second stream tube. This gas mixture was then assumed to flow downstream, react, and radiate in accordance with RESALE until $x = x_2$, the point where the next stream tube crossed the flame sheet. This process was continued until all of the stream tubes were absored at

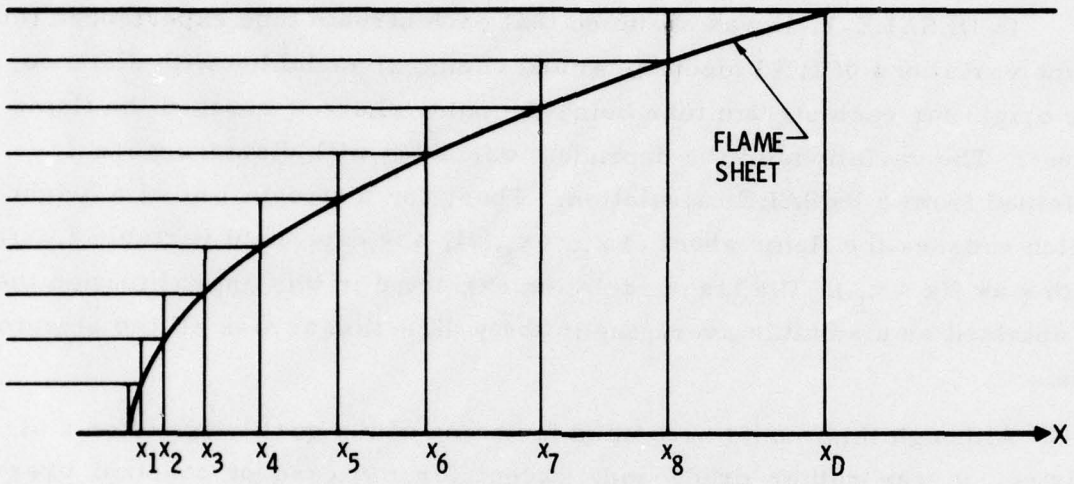

Fig. 2. DESALE-2 Mixing Model

$x = x_D$, the diffusion or mixing length. This model tends to exaggerate the thoroughness of the mixing process in that conditions interior to the flame sheet were assumed to be uniform in the y-direction. Nonetheless, it was believed that this would result in a tolerable approximation, which was probably no worse than the uncertainties associated with x_D and the reaction rates.

The initial conditions for the RESALE calculation in each segment were obtained by solving the equations for conservation of mass and momentum at each segment boundary for the assumed uniform conditions that would result from the instantaneous mixing of the incoming flows, that is, the jump conditions. At the time that DESALE-2 was developed, the interest was primarily in constant pressure flows. It was necessary to rederive the jump condition, including the equation of conservation of energy, to apply this model to other types of flows. It also became obvious that certain other improvements could be made with relatively little difficulty. These modifications resulted in DESALE-3.

In the derivation of DESALE-3, a slightly more realistic mixing geometry was adopted (Fig. 3). In this model, the primary and secondary streams were represented explicitly. The approximation that both streams were swallowed into the reaction zone at the same relative rate was retained, that is, x_D is the same for both streams. It was also assumed that flows at the nozzle exits were uniform. The options of considering either pressure prescribed as a function of x or area prescribed as a function of x were included. A subroutine was added to treat the latter case consistently and kept track of the gas outside of the reaction zone so that, when it reached the flame sheet, the gas properties were appropriate to the local area. For that part of the flow, it was assumed that the unreacted gas properties were determined by the one-dimensional isentropic flow relations.

In view of the fact that for constrained flows (prescribed area), sizeable changes in temperature, pressure, and velocity are expected when large

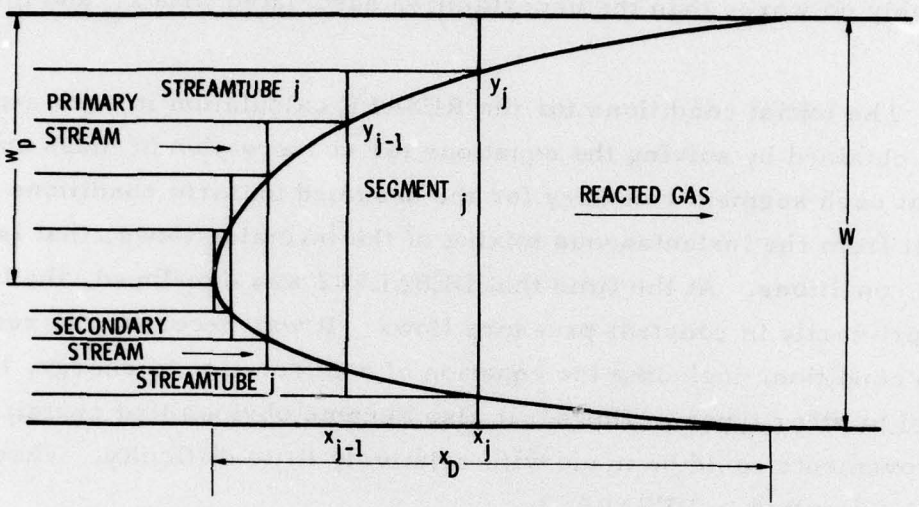

Fig. 3. DESALE-3 Mixing Model

amounts of chemical heat release occur, a further modification was introduced to account for these effects on the local rate of mixing. In the previous models (and, so far as is known to this writer, all other programmed mass addition models), the rate of mass addition is specified a priori in terms of the conditions upstream of the mixing zone. In DESALE-1 and 2, the flame sheet was assumed to be a parabola.

If the same approximation were used in DESALE-3, the shape of the flame sheet would be

$$\frac{y}{w_p} = \sqrt{\frac{x}{x_D}} \tag{1}$$

where the diffusion length x_D is given by

$$x_D = \frac{w_p^2 u}{D} \tag{2}$$

in accordance with laminar diffusion theory. Here, w_p is the primary nozzle semichannel height, u is the gas velocity, and D is a nominal diffusion coefficient. The latter may be approximated by

$$D = C \frac{p}{T^{3/2}} \tag{3}$$

where C is a constant that depends on the gas composition, p is the gas pressure, and T is the gas temperature. In all other programmed mass addition models, x_D is taken to be a constant evaluated at x = 0. In DESALE-3, x_D is allowed to vary to account for the local changes in mixing rate; thus, Eq. (1) is first rewritten as

$$x = \frac{x_D}{w_p^2} y^2 \tag{4}$$

If the desire is to calculate the shape of the boundary of the mixing zone in the j^{th} segment, at the beginning of that segment, $x = x_{j-1}$ and $y = y_{j-1}$ (Fig. 3). If the segment is sufficiently short, Eq. (4) can be approximated by the first few terms in a series expansion.

$$x = x_{j-1} + \left(\frac{dx}{dy}\right)_{j-1} (y - y_{j-1}) + \frac{1}{2}\left(\frac{d^2x}{dy^2}\right)_{j-1} (y - y_{j-1})^2 + \ldots \qquad (5)$$

If x_D were a constant, all derivatives higher than the second would be zero. In practice, x_D is a slowly varying function of x. With the variation of x_D within a segment and the derivatives higher than the second neglected and the results evaluated at $x = x_j$, the downstream edge of the j^{th} segment is

$$x_j = x_{j-1} + \frac{2x_{D_{j-1}}}{w_p^2} y_{j-1} (y_j - y_{j-1}) + \frac{x_{D_{j-1}}}{w_p^2} (y_j - y_{j-1})^2 \qquad (6)$$

Since y_j and y_{j-1} are given by the boundaries of the j^{th} stream stube, the downstream edge of the j^{th} segment is determined by means of Eq. (6). If x_D were constant, this result would correspond exactly to the usual parabolic variation. In DESALE-3, this result is modified by evaluating x_D locally with the use of Eqs. (2) and (3).

$$x_D(x) = C \frac{w_p^2 u_c(x) p_c(x)}{[T_c(x)]^{3/2}} \qquad (7)$$

where the subscript c refers to conditions in the reaction zone.

Within each segment, the solution is calculated with RESALE, just as in DESALE-2. The initial conditions for each segment are determined by applying the principles of conservation of mass, momentum, and energy

at each segment boundary (the jump conditions). For example, for the jump conditions at the end of the j-1'st segment (that is, the initial conditions for the j^{th} segment), the fluid in the j^{th} segment consists of the products of reaction in the j-1'st segment and the jth primary and secondary stream tubes. By the time the calculation has reached the j^{th} segment, the properties of these various streams have been determined. The initial conditions for the j^{th} segment is then determined by solving the algebraic equations for the conservation of mass, momentum, and energy across the segment boundary. The form of the solution depends on whether the prescribed pressure or prescribed area option is being used. In either case, the algebraic manipulation of the equations to obtain a solution is straightforward but tedious. The results are given in the Appendix.

One feature of the solution is worthy of discussion here. If the pressure is prescribed as a function of x, then the jump conditions must be solved, subject to the constraint of constant pressure. One finds, in fact, an explicit unique solution for this case. If the area is prescribed as a function of x, the jump conditions must be solved subject to the constraint of constant area. In that case, as in the analogous Rankine-Hugoniot shock jump conditions, there are two possible solutions to the problem: a strong solution and a weak solution. Since DESALE-3 is restricted to uniform initial flows and, in practical devices, the nozzle flows are supersonic, it is easy to determine which solution is appropriate. When the nozzle exit profiles are nonuniform, the situation becomes more complicated (see discussion of DESALE-5).

Soon after DESALE-3 become operational, considerable interest developed in the possibility of treating blockage in a computer model. For practical reasons, there is always at least a small amount of blockage, or land area, between adjacent nozzles. For some nozzle designs, for example, axisymmetric nozzles, appreciable blockage is unavoidable. In certain applications, large amounts of blockage may be built into the nozzle design

deliberately (for example, when there is a large amount of heat release). In the latter case, it would be desireable to be able to determine just how much blockage to use.

There are various ways in which blockage may occur in the nozzle design. In general, it may exist between the primary and secondary nozzles or, the primary and secondary nozzles may be continguous and the blockage may exist between separate nozzle pairs. For the former case, there is no mixing or reaction until the primary and secondary streams have merged. At that point the flow proceeds as in the no-blockage case, but with initial conditions adjusted to account for the larger flow area. DESALE-4 was developed to treat the latter case.

Since the accurate treatment of blockage requires the consideration of detached recirculating flows, very elaborate numerical computations would be required to obtain unequivocal results. Such an approach would be inconsistent with the level of approximation employed in the programmed mass addition models. A more ad hoc approach therefore was chosen.

It is well known that in detached, recirculating flows, the size and shape of the recirculation zone is significantly influenced by viscous effects. It is well known also that, when two chemically reactive free jets are allowed to mix and react, the area occupied by the flow may grow to be very large if the heat release resulting from the chemical reaction is large. The point of view taken in the present model is that the latter mechanism is the dominant one. Whereas this obviously will not be true in the limit of small heat release, that limit is not anticipated to be important for practical chemical laser devices.

Consequently, it is assumed in this model that as the primary and secondary jets leave their respective nozzles, they mix and react. As heat is released, the flow area expands (Figs. 4a, 4b, and 4c). Since the blockage provides room for the expansion, the flow acts like a free jet. It is assumed therefore that until the flow reaches some point where the blockage area is

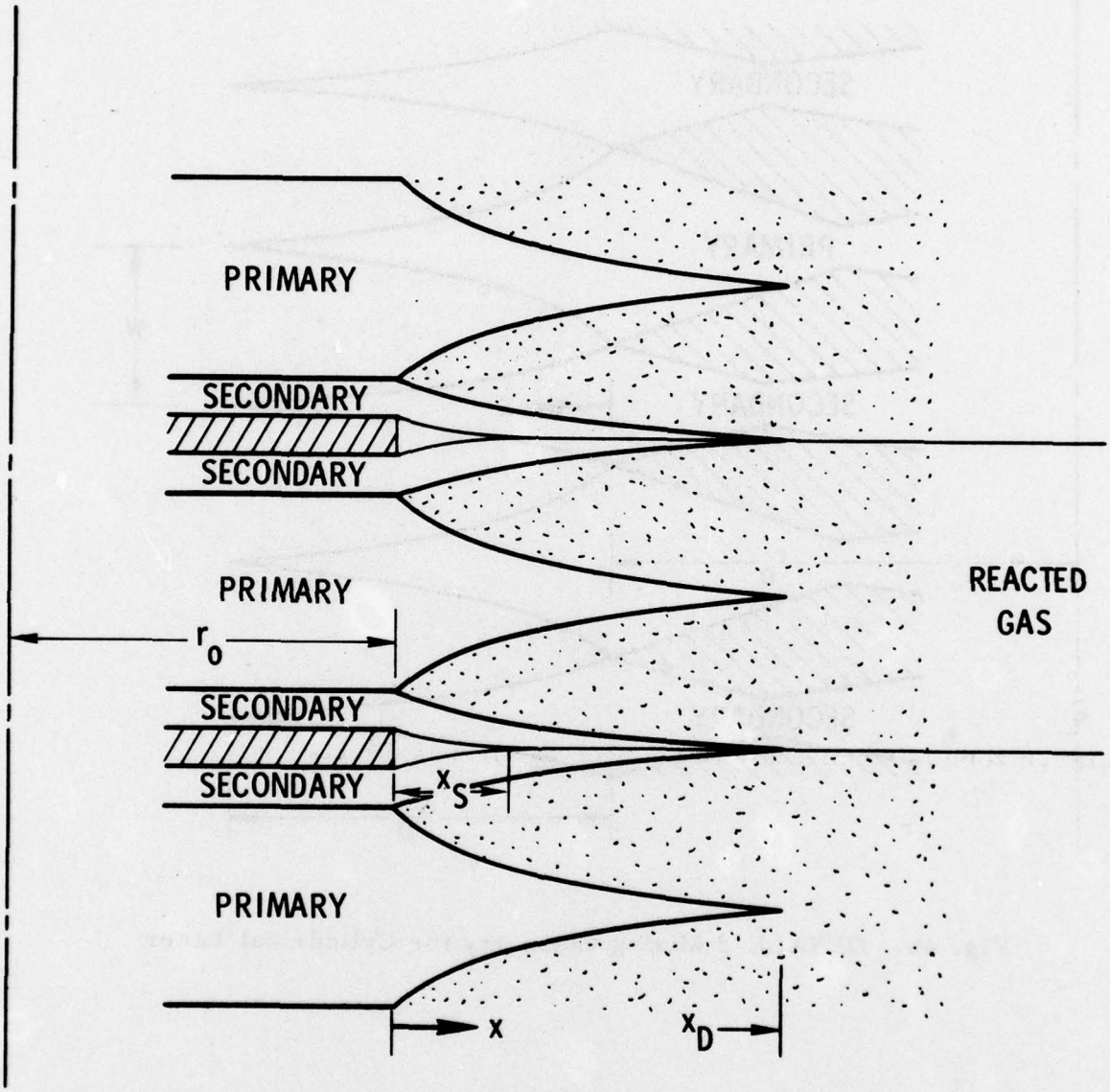

Fig. 4a. DESALE-4 Mixing Model with Blockage

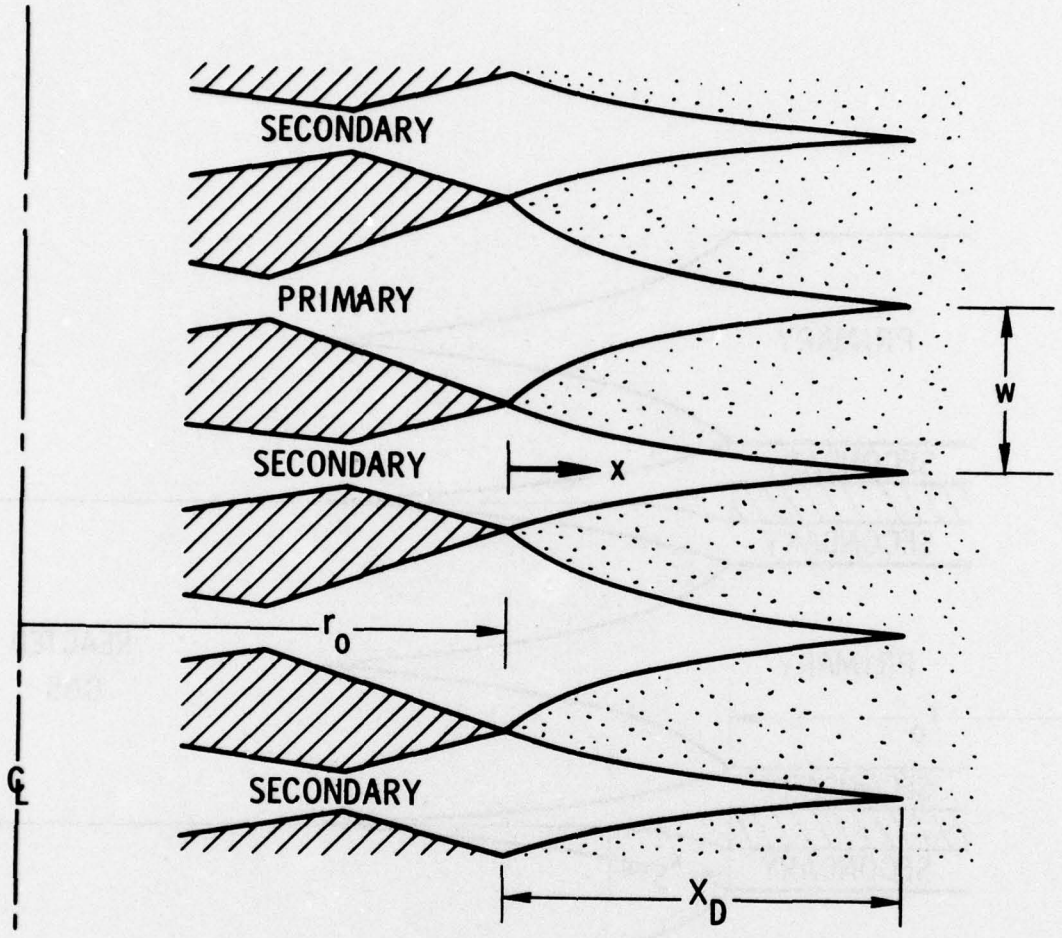

Fig. 4b. DESALE-3 Mixing Geometry for Cylindrical Laser

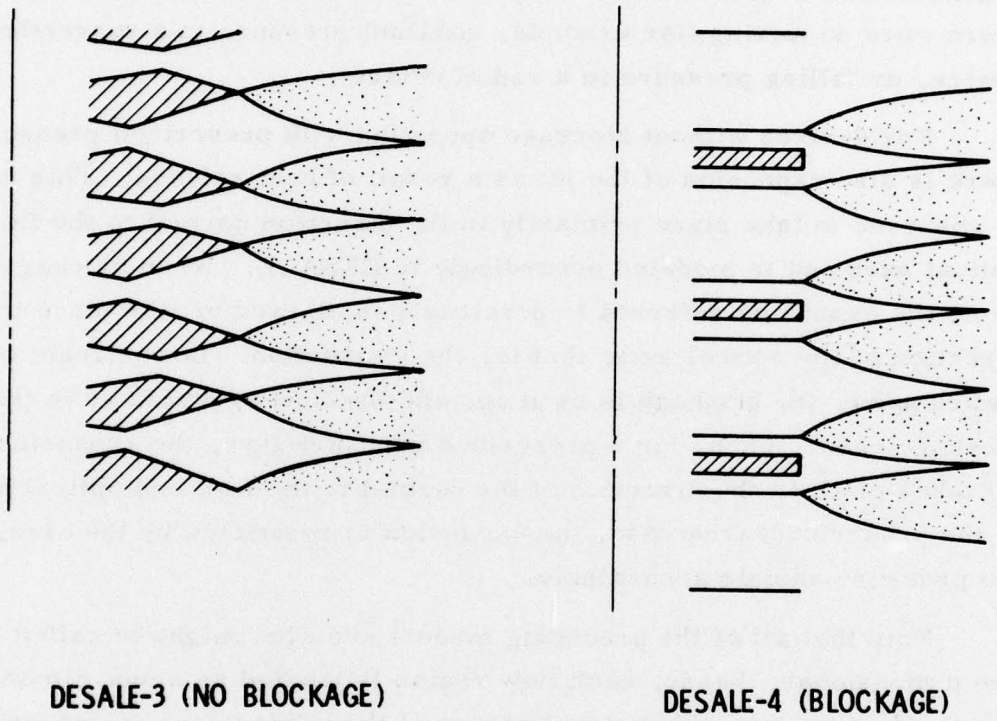

Fig. 4c. DESALE-3 AND DESALE-4 Mixing Geometry for Cylindrical Laser

used up x_s, the mixing and reaction takes place as in a free jet. The point x_s is designated the "switch-point." It is that point at which the sum of the primary, secondary, and reacted flow stream tube areas become equal to the total available flow area. Note that the term "free jet" is used here in a generalized sense, that is, the pressure field is whatever it would be if there were no mixing (for example, constant pressure in a conventional device, or falling pressure in a radial device).

For devices without blockage operating with prescribed pressure, there is also expansion of the jet as a result of heat release. This expansion is observed to take place primarily in the direction normal to the flow and optical axes and is modeled accordingly in DESALE. When blockage is present, the expansion referred to previously is allowed to take place in the direction of the optical axis, that is, the y direction. Downstream of the switch point, the blockage is used up, and the flow proceeds as in the no-blockage case. Thus, for a prescribed pressure flow, the expansion of the jet takes place in the direction of the normal to the flow and optical axes. In the prescribed-area case, the expansion is restricted by the area, and the pressure adjusts accordingly.

Note that all of the preceding models are what might be called quasi-one dimensional, that is, each flow region is treated as a one-dimensional flow. The true two-dimensional nature of the mixing zone is approximated by providing programmed mass addition into the mixing zone, which grows in width in approximate correspondence with the local diffusion rate.

By the time that DESALE-4 had been developed, it was clear that the nonuniform initial conditions from nozzle boundary layers could have a significant effect on laser performance. The fully two-dimensional codes that had been developed by that time were capable of treating these more complicated problems but with run times that were one-half to a full order of magnitude or more longer than the programmed mass addition codes.

The cost of parametric and extensive preliminary design computation with the more sophisticated codes was prohibitive, and yet, the accuracy of the existing more rapid programmed mass addition codes was questionable. Although the need for a simple but adequate code was obvious, it appeared that the quasi-one-dimensional approach might have to be pushed beyond reasonable limits if applied to the problem of nonuniform initial conditions. Although this is undoubtedly a reasonable concern, certain aspects of the problem of nonuniform initial conditions indicate that an appropriate programmed mass addition model might indeed reasonably model the essential features of the nonuniformities. After all, the programmed mass addition models adequately modeled the two-dimensional mixing when the initial profiles were uniform.

It appeared that the primary effects of the nozzle boundary layers were to significantly affect the temperature, F-atom concentration (effects of wall catalycity), and velocity of the first stream tubes that mixed. In many cases of practical importance, the nozzle wall temperatures are much higher than the core flow, with the result that the reaction may proceed much faster at the beginning of the reaction zone than if the gas temperature were uniform. Similarly, if F-atom recombination on the nozzle walls is significant, the reactions at the beginning of the mixing zone may be appreciably inhibited.

From considerations such as these, it became clear that these effects at least could be approximately accounted for by only a slight modification to DESALE-4. Since the approach taken in the DESALE series of models was based on the assumption that successive pairs of primary and secondary stream tubes entered the mixing zone in a scheduled manner, the modification required involved only a slight complication in bookkeeping. That is, the effect of nonuniform initial profiles could be accounted for in the DESALE type of model by simply allowing the gas properties in each stream tube to differ in accordance with the specified initial profiles. The computation of

the jump conditions and the flow in each segment is therefore independent of the initial nonuniformities. The only complications are the increased amounts of input data and computer internal storage and data retrieval operations. Implementation of this concept, in fact, has shown that computation time is generally increased by less than 5%.

In the implemenation of this model, a problem was discovered in the calculation of the jump conditions for the prescribed area option. In that case, it was found that to obtain the velocity downstream of the segment boundary, a quadratic equation had to be solved (Appendix), which resulted in two possible solutions. An analytical examination of the equations indicated that the appropriate solution could be identified if the Mach numbers of the incoming streams were either all subsonic or all supersonic. In other cases, it was necessary to examine the entropy for each solution. The proper solution was the one that provided the least increase in system entropy. In applying these results, it was sometimes found that larger than normal jumps in Mach number occurred at those segment boundaries across which the reacted zone Mach number went from subsonic to supersonic. Auxilliary analytical investigations resulted in the conclusion that this was an artifact related to the assumption of uniform profiles in the reacted zone. Numerical experimentation indicated that, when these jumps occurred, they appeared as transients that only slightly affected the overall results.

III. ILLUSTRATIVE EXAMPLES

Two illustrative examples are presented in this section. The first is a constant-pressure case without blockage with relatively mild nonuniformities, that is, cool walls. The purpose of this example is to illustrate the changes in the qualitative nature of the solution that result from nozzle boundary layers for conditions where minimal effects are expected. This example provides a reference for later cases where much stronger effects are observed.

Note that, when comparing results of calculations for a given geometry with uniform and nonuniform initial profiles, there is no unambiguous way of making this comparison. In this study, the choice has been made to match the centerline values of all of the variables for both the uniform and nonuniform initial profiles, which results in a lower mass flow for the nonuniform initial profile calculation. This discrepancy can be accounted for by comparing specific powers rather than powers.

The conditions for the constant-pressure calculation are as follows: cavity pressure $p = 5.7$ Torr, semichannel height $w = 0.127$ cm, number of semichannels $n_{sc} = 1500$, distance between mirrors $L = 190.5$ cm, F-atom mass fraction $\alpha = 0.9$, diluent (He/F_{2_0}) $\beta = 10$, fuel ratio (H_2/F_{2_0}) $N = 5$, plenum pressure $p_0 = 1$ atm, and wall temperature = 300 K. The primary and secondary velocity, temperature, and concentration profiles are shown in Fig. 5. These profiles were obtained from boundary-layer calculations, subject to the boundary condition of a catalytic wall.

The specific power is shown as a function of mirror length in Fig. 6. Since the walls are hotter than the core flow, the pumping reactions proceed faster in the nonuniform case. For this case, a slightly higher specific power is achieved with a somewhat smaller lasing zone before collisional deactivation sets in to quench the lasing. Note that the closeness of these calculations is fortuitous and is not generally expected for other initial conditions.

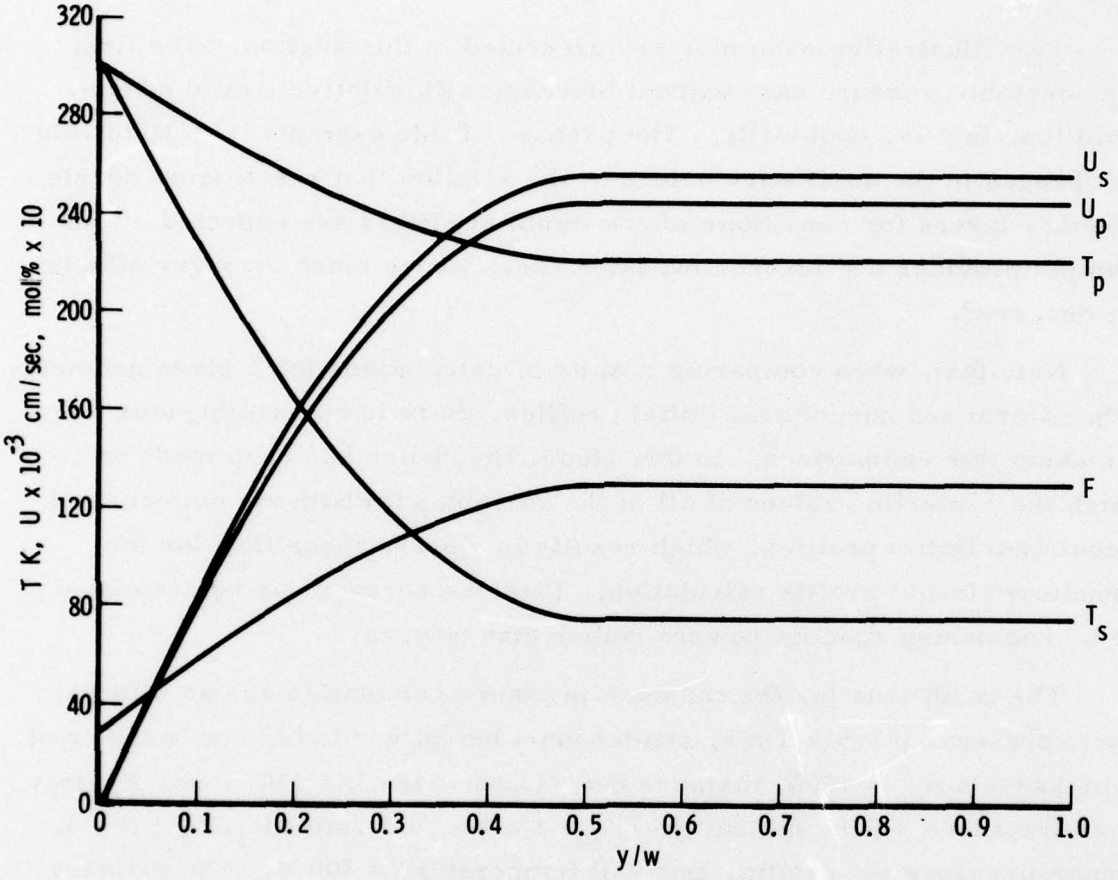

Fig. 5. Initial Profiles. $w_p = 0.11392$ cm, $w_s = 0.01308$ cm

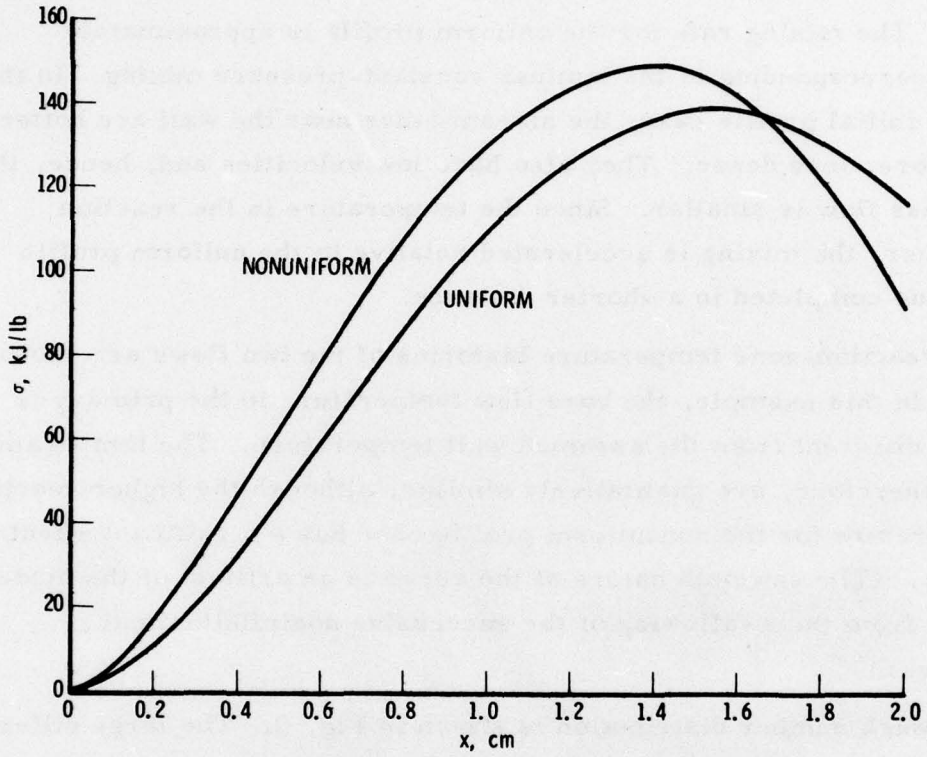

Fig. 6. DESALE-5 Cold-Reaction Laser Performance. Constant pressure, p_o = 1 atm, p = 5.7 Torr, w = .127 cm, n_{sc} = 1500, L = 190.5 cm α = 0.9, β = 10, N = 5 (core).

Some insight into the reasons for this behavior can be obtained by examining the behavior of some other pertinent parameters. In Fig. 7, the relative rate of mass addition is plotted as a function of distance into the cavity. The mixing rate for the uniform profile is approximately parabolic, corresponding to the laminar constant-pressure mixing. In the nonuniform initial profile case, the stream tubes near the wall are hotter and, therefore, less dense. They also have low velocities and, hence, the relative mass flow is smaller. Since the temperature in the reaction zone is higher, the mixing is accelerated relative to the uniform profile case and thus completed in a shorter distance.

The reaction-zone temperature histories of the two flows are shown in Fig. 8. In this example, the core flow temperature in the primary is not greatly different from the assumed wall temperature. The temperature histories, therefore, are qualitatively similar, although the higher reaction zone temperature for the nonuniform profile case has a significant effect on the kinetics. (The sawtooth nature of the curve is an artifact of the model and results from the swallowing of the successive noninfinitesimal stream tubes.)

The Mach number distribution is shown in Fig. 9. The large differences in the early part of the mixing zone are the result of the low velocities in the boundary layers. Note that the ad hoc procedure described in the previous section for modifying the local mixing rate in accordance with local conditions is especially valuable here. With other programmed mass addition models, the mixing rate can be calculated on the assumption that two uniform streams mix with velocity, temperature, and pressure characteristic of the primary stream core flow. In the real case, the higher temperatures and lower velocities near the wall will provide for much more rapid diffusion, an effect that is approximately accounted for in the present model.

The use of the blockage portion of the model is illustrated in the second example. Conditions characteristic of a cold-reaction cylindrical laser

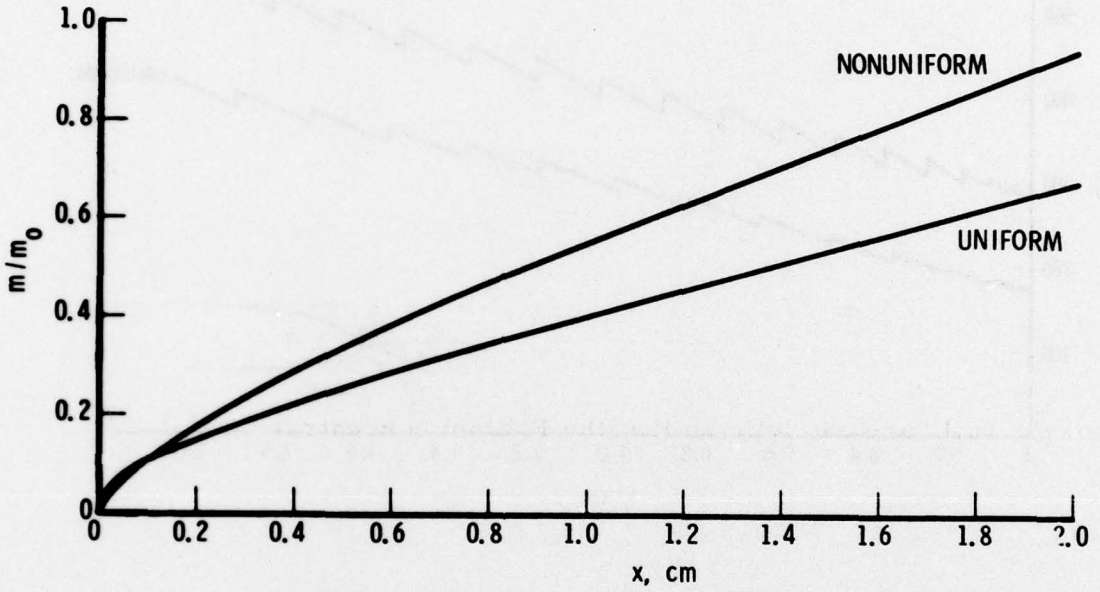

Fig. 7. Mixing Rate. Constant pressure, p = 5.7 Torr, w = .127 cm, n_{sc} = 1500, L = 190.5 cm, α = 0.9, β = 10, N = 5 (core).

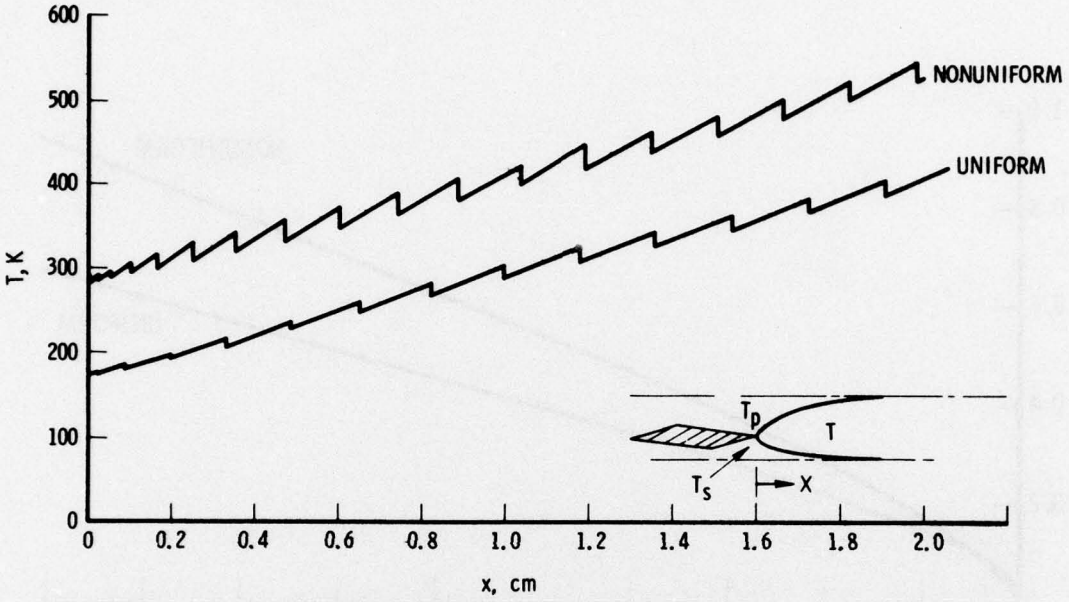

Fig. 8. Temperature Distribution. Constant pressure, p = 5.7 Torr, w = .127 cm, n_{sc} = 1500, L = 190.5 cm, p_o = 1 atm, α = 0.9, β = 10, N = 5 (core), T_p = 221 K, T_s = 74 K.

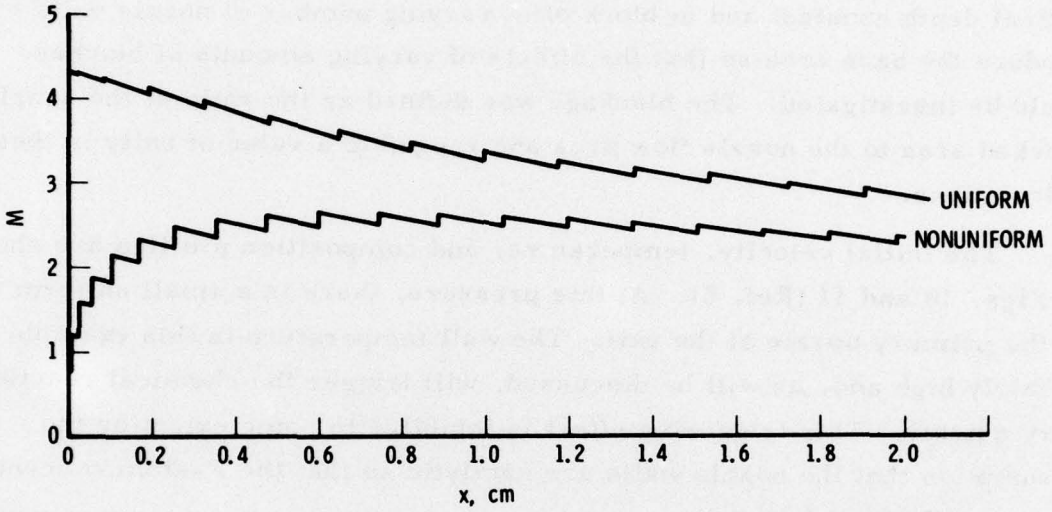

Fig. 9. Mach Number Distribution. Constant pressure, p = 5.7 Torr, w = .127 cm, n_{sc} = 1500, L = 190.5 cm, p_o = 1 atm, α = 0.9, β = 10, N = 5 (core).

are employed: p = 8.6 Torr, semichannel height = 1 mm, L = 5 cm, wall temperature = 550 K, α = 1.0, β = 13.6, and N = 6.8. The diameter of the device at the nozzle exit is 12 in. The choice was made to keep the total optical depth constant and to block off a varying number of nozzle exits to produce the base area so that the effects of varying amounts of blockage could be investigated. The blockage was defined as the ratio of the nozzle blocked area to the nozzle flow area and ranged to a value of unity in these calculations.

The initial velocity, temperature, and composition profiles are shown in Figs. 10 and 11 (Ref. 8). At this pressure, there is a small uniform core in the primary nozzle at the exit. The wall temperature in this example is fairly high and, as will be discussed, will trigger the chemical reactions very quickly. This triggering effect is inhibited to some extent by the assumption that the nozzle walls are catalytic so that the F-atom concentration near the wall is small.

In Fig. 12, the specific power profiles are compared for the case of zero and 30% blockage. For these conditions, a 50% increase in peak specific power occurs. The reasons for this behavior are explained by the temperature, pressure, and Mach number histories given in Figs. 13 through 15.

The temperature at the beginning of the reaction zone starts essentially at the wall temperature in both cases but drops rapidly, partly as a result of swallowing of cooler stream tubes and partly the radial expansion (Fig. 13). Eventually, the heat release that results from the chemical reaction becomes dominant, and the temperature increases. In the no-blockage case, the flow cannot expand to accommodate the heat release and the pressure rises, which further increases the rate of reaction and the temperature (Fig. 14). Eventually, the temperature and pressure become high enough to cause the collisional deactivation to quench the lasing. For the case of 30% blockage, the switch point occurs at about 1.1 cm. Upstream of that position, the flow

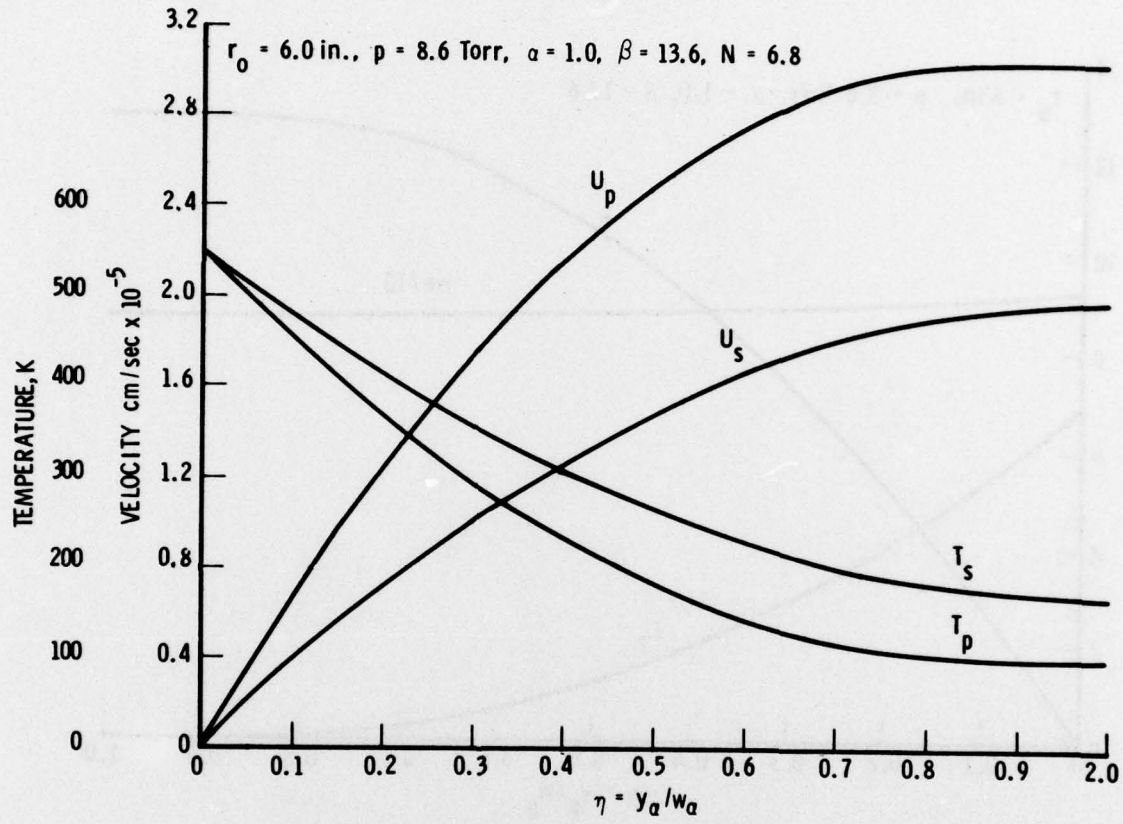

Fig. 10. Initial Velocity and Temperature Profiles. r_o = 6.0 in., p = 8.6 Torr, α = 1.0, β = 13.6, N = 6.8.

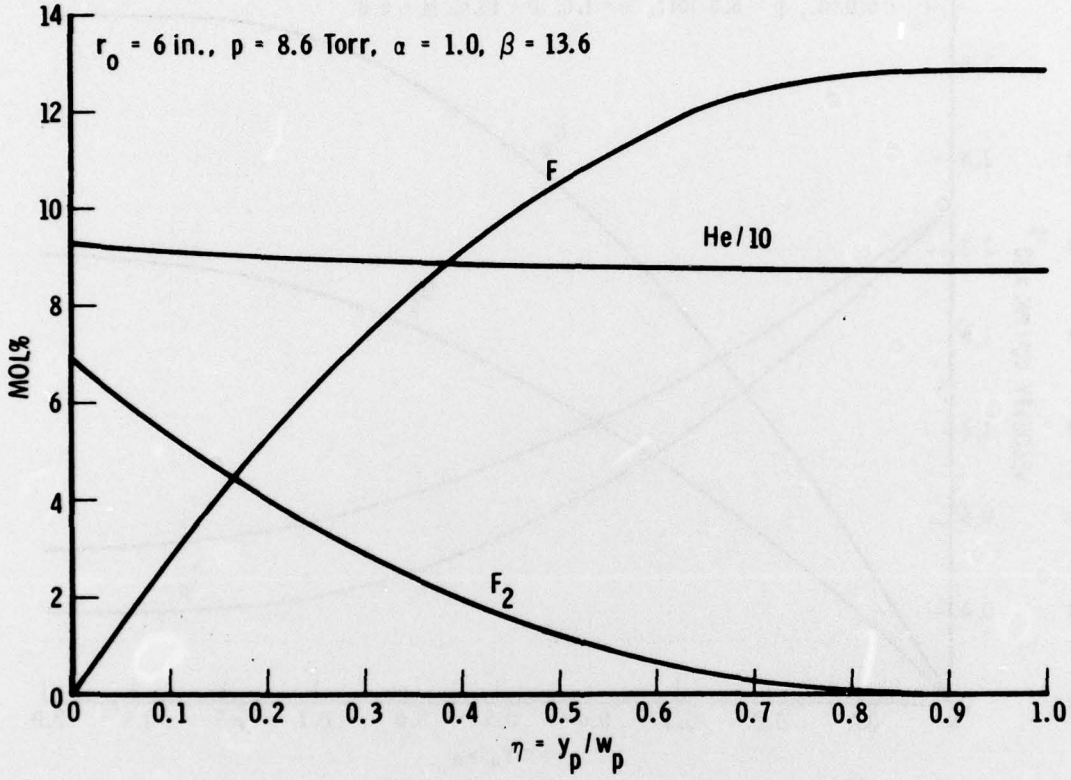

Fig. 11. Primary Nozzle Exit Composition Profiles. r_o = 6 in., p = 8.6 Torr, α = 1.0, β = 13.6.

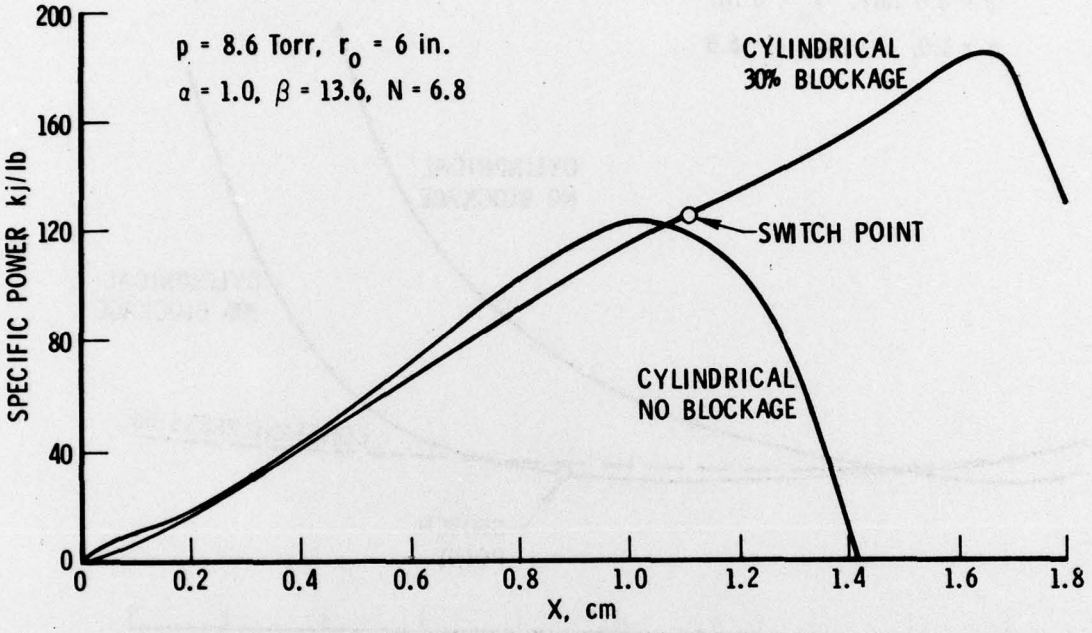

Fig. 12. Power Profiles. p = 8.6 Torr, r_o = 6 in, α = 1.0, β = 13.6, N = 6.8.

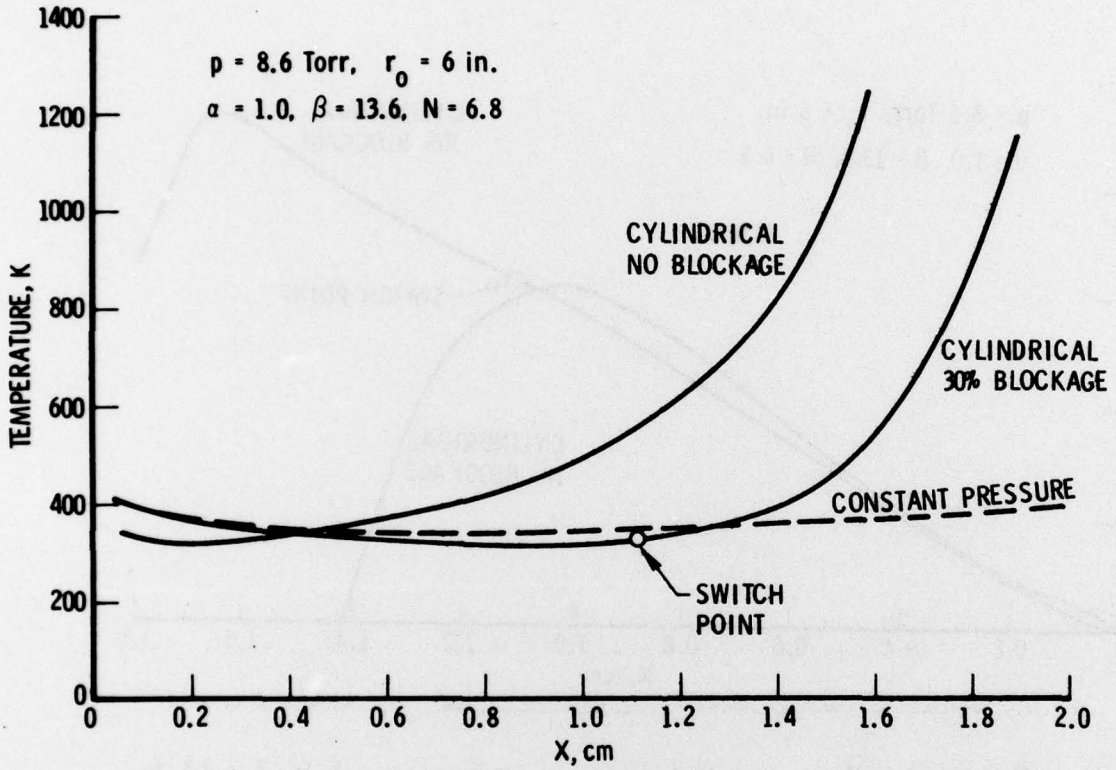

Fig. 13. Temperature Profiles. p = 8.6 Torr, r_o = 6 in., α = 1.0, β = 13.6, N = 6.8.

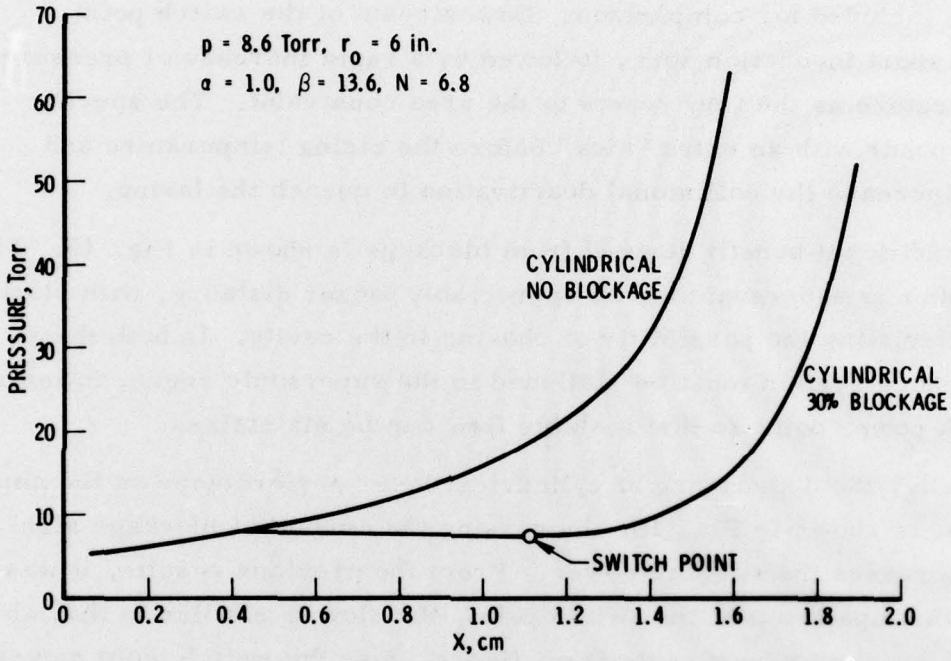

Fig. 14. Pressure Profile. p = 8.6 Torr, r_o = 6 in., α = 1.0, β = 13.6, N = 6.8.

expands to accommodate the heat release, the amount of expansion dicatated by the falling pressure field associated with a radial expansion with no heat release. Since the flow distances involved here are small compared to the nozzle exit radius, the pressure falls only slightly. The constant pressure solution is included for comparison. Downstream of the switch point, there is a short incubation zone, followed by a rapid increase of pressure and temperature as the flow reacts to the area constraint. The specific power responds with an extra "kick" before the rising temperature and pressure increase the collisional deactivation to quench the lasing.

An additional benefit derived from blockage is shown in Fig. 15. The Mach number is supersonic for an appreciably longer distance, with blockage thereby alleviating the possibility of choking in the cavity. In both these cases, a shock system must be stationed in the supersonic region downstream of the peak power point so that a stable flow can be maintained.

Finally, the dependence of cylindrical laser performance on the amount of blockage is shown in Fig. 16. Increasing the amount of blockage significantly increases the specific power. From the previous results, it was indicated that upstream of the switch point, the flow is similar to that which exists in a constant pressure device. Hence, once the switch point moves downstream of the peak power point, there is no further gain from increasing blockage. Note that the decreasing power with increasing blockage is an artifact related to the way in which the blockage was varied in this calculation, that is, increasing blockage was obtained by decreasing the nozzle exit area with the total available flow area held fixed. If the nozzle exit area were fixed and the length of the device were allowed to grow, the power curve would be similar in shape to the specific power curve. The strong effect of blockage on lasing zone length is apparent. For this case, a doubling of the lasing zone length is possible with about 80% blockage.

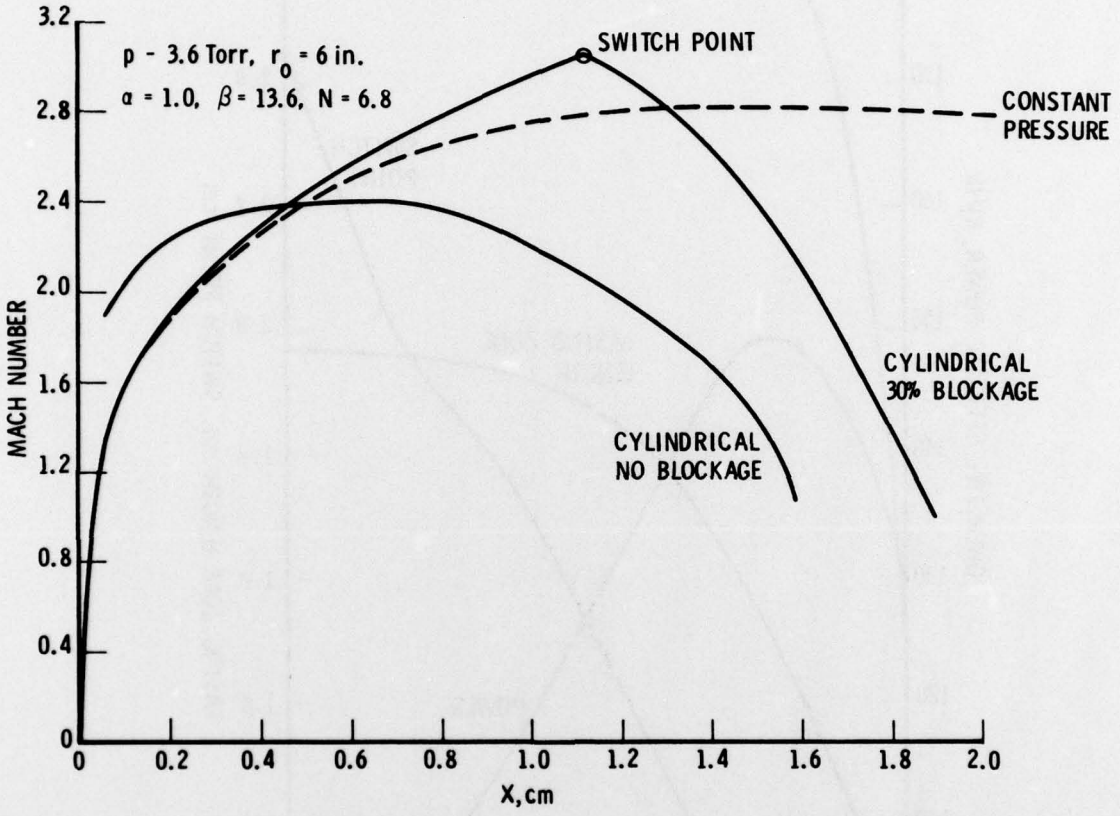

Fig. 15. Mach Number Profile. p = 3.6 Torr, r_o = 6 in., α = 1.0, β = 13.6, N = 6.8.

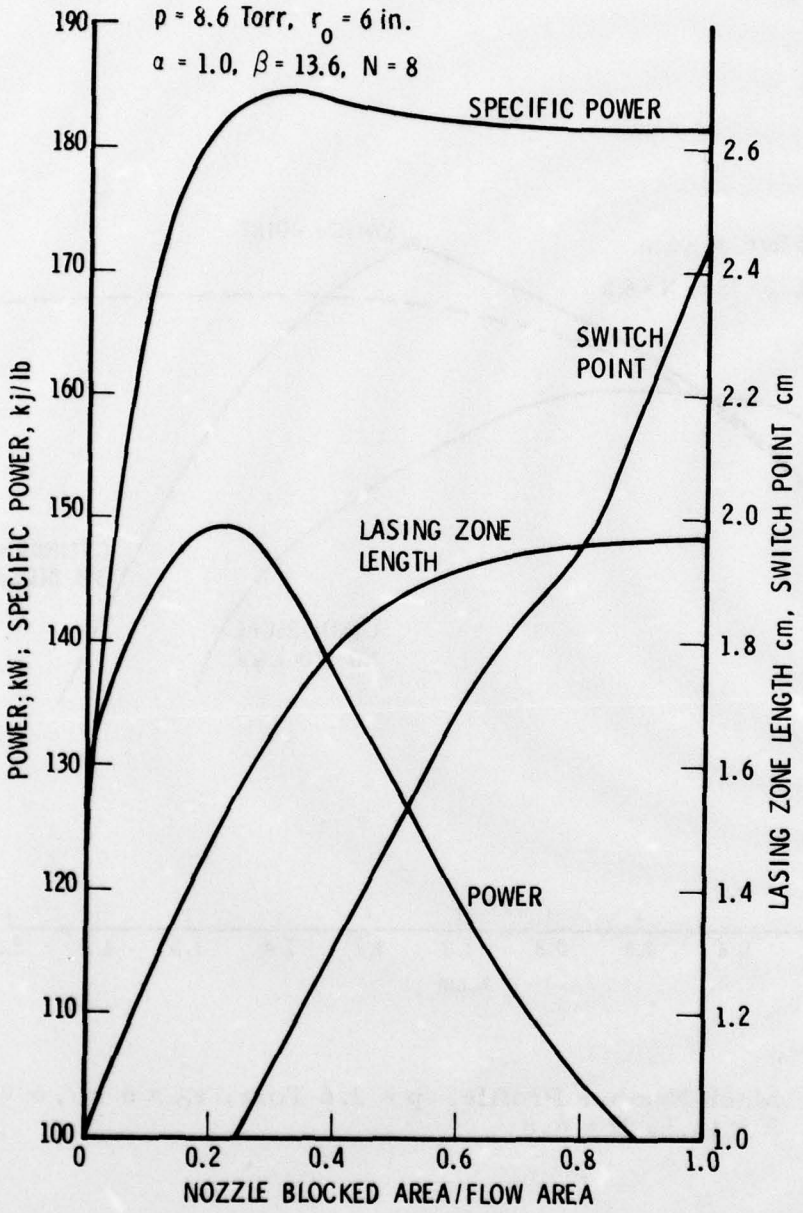

Fig. 16. Cylindrical Laser Performance versus Blockage. p = 8.6 Torr, r_o = 6 in., α = 1.0, β = 13.6, N = 8.

IV. CONCLUSIONS

A description has been given of the development of a comprehensive quasi-one dimensional model for calculating the performance of cw chemical lasers. The model, DESALE-5, is one dimensional in the sense that each stream tube is treated one dimensionally. Some of the two-dimensional aspects of the flow are treated in a semiquantitative way. In particular, the two-dimensional character of the mixing process is approximated by scheduling the rate of addition of reactants to the mixing zone. In this regard, the present model contains an improvement over other programmed mass addition models since the rate of mass addition is determined by the local values of the diffusion coefficient rather than the initial value.

DESALE-5 includes an option that permits the consideration of blockage in an approximate but qualitatively reasonable way. Illustrative calculations indicate that the effects of blockage can be significant both in terms of power and lasing zone length. Furthermore, these results indicate that there is an optimum amount of blockage for each set of operating conditions.

DESALE-5 also permits the consideration of nonuniform initial profiles resulting from, for example, nozzle boundary layers by assigning to each incoming stream tube the appropriate flow properties. Calculations performed so far indicate trends that are consistent with expectations. Detailed comparisons with fully two-dimensional models have yet to be made. Inclusion of the nonuniform initial profiles has had only a minor effect on the computation time. Running times typically have been found to be in the range of 25 to 40 sec on a CDC 7600, including both blockage and nonuniform initial profiles.

REFERENCES

1. K. J. Spencer, T. A. Jacobs, H. Mirels, and R.W.F. Gross, "Continuous-Wave Chemical Laser," Int. J. Chem. Kinetics, 1 (5), 493-494 (1969).

2. R. Hofland and H. Mirels, "Flame Sheet Analysis of CW Diffusion-Type Chemical Laser, II: Coupled Radiation," AIAA J. 10, 1271-1280 (1972).

3. G. Emanuel, RESALE-1: A Chemical Laser Computer Program, TR-0172(2776)-1, The Aerospace Corporation, El Segundo, Calif. (15 March 1972).

4. J. Thoenes, A. J. McDanal, A. W. Ratliff, and S. D. Smith, Chemical Laser Analysis Development, RK-CR-73-2, Lockheed Missiles & Space Co. (October 1973).

5. R. Tripodi, L. J. Coulter, B. R. Bronfin, and L. S. Cohen, "Coupled Two-Dimensional Computer Analysis of CW Chemical Mixing Lasers," AIAA J. 13, 776-784 (1975).

6. E. B. Turner, G. Emanuel, and R. L. Wilkins, The NEST Chemistry Computer Program, TR-0059(6240-20)-1, The Aerospace Corporation, El Segundo, Calif. (30 July 1970).

7. W. D. Adams, E. B. Turner, J. F. Holt, D. G. Smith, and H. Mirels, The RESALE Chemical Laser Computer Program, TR-0075(5530)-5, The Aerospace Corporation, El Segundo, Calif. (20 February 1975).

APPENDIX

JUMP CONDITIONS

The jump conditions are obtained by solving the equations for the conservation of mass, momentum, and energy for an assumed uniform condition immediately downstream of a segment boundary. The flow approaching the segment boundary on the upstream side consists of an unreacted primary stream tube (subscript a), an unreacted secondary stream tube (subscript b), and a reacted stream tube for the upstream segment (subscript c; absent at x = 0). There are two sets of jump conditions, depending on whether the jump occurs in a region of prescribed pressure or prescribed area. In the former case, the conservation equations are solved, subject to the constraint of constant pressure across the segment boundary; in the latter case, the constraint is constant area.

A. CONSTANT-PRESSURE JUMP CONDITIONS

$$u_{c_j} = \frac{\dot{m}_{a_j}}{\dot{m}_{c_j}} u_{a_j} + \frac{\dot{m}_{b_j}}{\dot{m}_{c_j}} u_{b_j} + \frac{\dot{m}_{c_{j-1}}}{\dot{m}_{c_j}} u_{c_{j-1}} \tag{A-1}$$

$$h_{c_j} = \frac{\dot{m}_{b_j}}{\dot{m}_{c_j}} \left(h_{a_j} + \frac{1}{2} u_{a_j}^2\right) + \frac{\dot{m}_{b_j}}{\dot{m}_{c_j}} \left(h_{b_j} + \frac{1}{2} u_{b_j}^2\right)$$

$$+ \frac{\dot{m}_{c_{j-1}}}{\dot{m}_{c_j}} \left(h_{c_{j-1}} + \frac{1}{2} u_{c_{j-1}}^2\right) - \frac{1}{2} h_{c_j}^2 \tag{A-2}$$

$$\rho_{c_j} = \frac{p}{R_{c_j} T_{c_j}} \tag{A-3}$$

$$A_{c_j} = \frac{m_{c_j}}{\rho_{c_j} u_{c_j}} \tag{A-4}$$

B. CONSTANT-AREA JUMP CONDITIONS

$$u_{c_j} = B_j \pm \sqrt{B_j^2 - C_j} \tag{A-5}$$

where

$$B_j = \frac{\gamma_{c_j}}{m_{c_j}(\gamma_{c_j}+1)} \left(P_{a_j} A_{a_j} + m_{a_j} u_{a_j} + P_{b_j} A_{b_j} + P_{c_{j-1}} A_{c_{j-1}} + m_{c_{j-1}} u_{c_{j-1}} \right) \tag{A-6}$$

$$C_j = \frac{2}{m_{c_j}} \left(\frac{\gamma_{c_j} - 1}{\gamma_{c_j} + 1} \right) \left[m_{a_j} \left(h_{a_j} + \frac{1}{2} u_{a_j}^2 \right) + m_{b_j} \left(h_{b_j} + \frac{1}{2} u_{b_j}^2 \right) + m_{c_{j-1}} \left(h_{c_{j-1}} + \frac{1}{2} u_{c_{j-1}}^2 \right) \right] \tag{A-7}$$

The choice of sign in Eq. (A-5) is made according to which solution gives the smallest increase in system entropy.

$$T_{c_j} = \frac{1}{2} \left(\frac{\gamma_{c_j} + 1}{\gamma_{c_j} - 1} \right) \frac{C_j}{C_{p_j}} - \frac{u_{c_j}^2}{2 C_{p_{c_j}}} \tag{A-8}$$

$$A_{c_j} = \frac{j}{n} A \tag{A-9}$$

$$p_{c_j} = \frac{\dot{m}_{c_j} R_{c_j} T_{c_j}}{u_{c_j} A_{c_j}} \qquad \text{(A-10)}$$

These equations can be simplified somewhat for DESALE-3 and DESALE-4 (uniform initial profiles).

LABORATORY OPERATIONS

The Laboratory Operations of The Aerospace Corporation is conducting experimental and theoretical investigations necessary for the evaluation and application of scientific advances to new military concepts and systems. Versatility and flexibility have been developed to a high degree by the laboratory personnel in dealing with the many problems encountered in the nation's rapidly developing space and missile systems. Expertise in the latest scientific developments is vital to the accomplishment of tasks related to these problems. The laboratories that contribute to this research are:

Aerophysics Laboratory: Launch and reentry aerodynamics, heat transfer, reentry physics, chemical kinetics, structural mechanics, flight dynamics, atmospheric pollution, and high-power gas lasers.

Chemistry and Physics Laboratory: Atmospheric reactions and atmospheric optics, chemical reactions in polluted atmospheres, chemical reactions of excited species in rocket plumes, chemical thermodynamics, plasma and laser-induced reactions, laser chemistry, propulsion chemistry, space vacuum and radiation effects on materials, lubrication and surface phenomena, photosensitive materials and sensors, high precision laser ranging, and the application of physics and chemistry to problems of law enforcement and biomedicine.

Electronics Research Laboratory: Electromagnetic theory, devices, and propagation phenomena, including plasma electromagnetics; quantum electronics, lasers, and electro-optics; communication sciences, applied electronics, semiconducting, superconducting, and crystal device physics, optical and acoustical imaging; atmospheric pollution; millimeter wave and far-infrared technology.

Materials Sciences Laboratory: Development of new materials; metal matrix composites and new forms of carbon; test and evaluation of graphite and ceramics in reentry; spacecraft materials and electronic components in nuclear weapons environment; application of fracture mechanics to stress corrosion and fatigue-induced fractures in structural metals.

Space Sciences Laboratory: Atmospheric and ionospheric physics, radiation from the atmosphere, density and composition of the atmosphere, aurorae and airglow; magnetospheric physics, cosmic rays, generation and propagation of plasma waves in the magnetosphere; solar physics, studies of solar magnetic fields; space astronomy, x-ray astronomy; the effects of nuclear explosions, magnetic storms, and solar activity on the earth's atmosphere, ionosphere, and magnetosphere; the effects of optical, electromagnetic, and particulate radiations in space on space systems.

THE AEROSPACE CORPORATION
El Segundo, California